




## REGULAR ARTICLE

### Electronic Structure and Thermoelectric Properties of $\beta$ -Ag<sub>8</sub>GeSe<sub>6</sub> Crystal Calculated by DFT

I.V. Semkiv<sup>1,\*</sup> , H.A. Ilchuk<sup>1</sup>, M. Pawłowski<sup>2,†</sup>, N.Yu. Kashuba<sup>1</sup>, N.T. Pokladok<sup>1</sup>, A.I. Kashuba<sup>1,‡</sup>

<sup>1</sup> Department of General Physics, Lviv Polytechnic National University, 79013 Lviv, Ukraine

<sup>2</sup> Faculty of Physics, Warsaw University of Technology, 00-662 Warsaw, Poland

(Received 20 June 2024; revised manuscript received 14 August 2024; published online 27 August 2024)

The  $\beta$ -Ag<sub>8</sub>GeSe<sub>6</sub> crystallizes in the orthorhombic structure ( $Pma2_1$  space group) at room temperature and is studied in the framework of density functional theory. The theoretical first-principle calculations of the electronic band structure, density of states, Seebeck coefficient, power factor, electrical conductivity and effective mass of the electron and hole of  $\beta$ -Ag<sub>8</sub>GeSe<sub>6</sub> crystal are estimated by the generalized gradient approximation (GGA). A Perdew–Burke–Ernzerhof functional (PBE) was utilized. The effective mass of the electrons and holes was calculated based on the electronic band structure. Seebeck coefficient, power factor and electrical conductivity as functional temperature are studied and discussed. All obtained values at room temperature are compared with known experimental results.

**Keywords:** Density functional theory, Electron band structure, Effective mass, Density of state, Seebeck coefficient, Power factor.

DOI: [10.21272/jnep.16\(4\).04036](https://doi.org/10.21272/jnep.16(4).04036)

PACS number: 71.20. – b

## 1. INTRODUCTION

Ag<sub>8</sub>GeSe<sub>6</sub> compound belongs to the argyrodite-type materials and is after the name of its natural mineral Ag<sub>8</sub>GeSe<sub>6</sub> [1]. At low temperatures, Ag<sub>8</sub>GeSe<sub>6</sub> crystal has  $\alpha$ -modification ( $T \leq 271$  K), but information about structure and lattice parameters is still lacking at present. At room temperatures, the crystal structure of Ag<sub>8</sub>GeSe<sub>6</sub> belongs to the orthorhombic space group  $Pmn2_1$  (No. 31) ( $271 \leq T \leq 323$  K). And at high temperatures was observed high symmetry face-centered cubic structure ( $\gamma$ ) of Ag<sub>8</sub>GeSe<sub>6</sub> ( $F-43m$  space group,  $T \geq 350$  K). Need be noted that the literature has information about the present  $\varepsilon$ -phase in Ag<sub>8</sub>GeSe<sub>6</sub> crystal, witch observed between 323 and 350 K. The structural information and detailed lattice parameters of  $\varepsilon$  phase are unknown at present, too. But, we found different information about the structure transition between these modifications of Ag<sub>8</sub>GeSe<sub>6</sub> argyrodite. In Ref. [2] was reported that temperatures of phase transition are 271 and 323 K, and in Refs. [3, 4] –  $-4^\circ\text{C}$  ( $\sim 269$  K) and  $48^\circ\text{C}$  ( $\sim 321$  K), respectively for  $\alpha \rightarrow \beta$  and  $\beta \rightarrow \gamma$  phase transitions. Information about the  $\varepsilon$ -modification of Ag<sub>8</sub>GeSe<sub>6</sub> was reported in Ref. [5]. As result, in this work gives results of the studies of fundamental properties of the  $\beta$ -Ag<sub>8</sub>GeSe<sub>6</sub> between 271 and 321 K to exclude the effect of a possible structural transition.

In the literature we observed same information about the fundamental physical properties of  $\beta$ -Ag<sub>8</sub>GeSe<sub>6</sub>. The study of fundamental thermodynamics properties based on different thermal analysis and X-ray diffraction data is given in [1, 6, 7] and thermoelec-

tric properties in [8, 9]. Also, we will be noted that studies of the electronic energy spectra of  $\beta$ -Ag<sub>8</sub>GeSe<sub>6</sub> crystal are absent in the literature.

Ag and Cu-contained argyrodites are defined as chalcogenides crystallized in tetrahedrally close-packed structures and attract high attention as promising thermoelectric materials [10-13]. The most important electronic characteristics of a crystal for their thermoelectric and photovoltaic applications are the bandgap, the effective electron mass, Seebeck coefficient, and the coefficients of electric and thermal conductivities [11, 14].

The ability to determine the electronic and thermoelectric characteristics of materials by using theoretical methods is promising for the evaluation of their possible practical applications. In the present work, the electronic band structure, density of states, electron and hole effective mass, Seebeck coefficient, power factor and electrical conductivity of the  $\beta$ -Ag<sub>8</sub>GeSe<sub>6</sub> crystal have been calculated for the first time.

## 2. METHODS OF CALCULATION

The theoretical calculations were performed within the framework of the density functional theory (DFT). To calculate the properties of  $\beta$ -Ag<sub>8</sub>GeSe<sub>6</sub> crystal, a crystalline lattice with the basal parameters given below in Table 1 was used. To describe the exchange-correlation energy of the electronic subsystem, we used a functional taken in the approximation of generalized gradient (GGA) and Perdew–Burke–Ernzerhof (PBE) parameterization [15]. Ultrasoft Vanderbilt's pseudopotentials [16] served as ionic potentials.

\* Correspondence e-mail: [ihor.v.semkiv@lpnu.ua](mailto:ihor.v.semkiv@lpnu.ua)

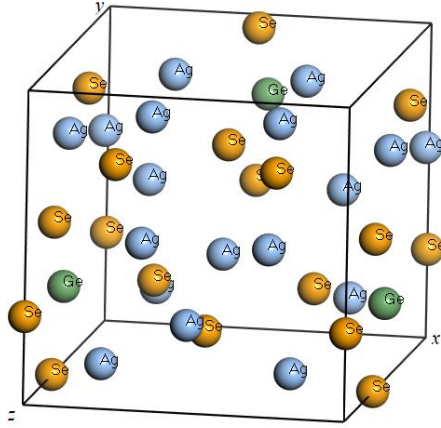
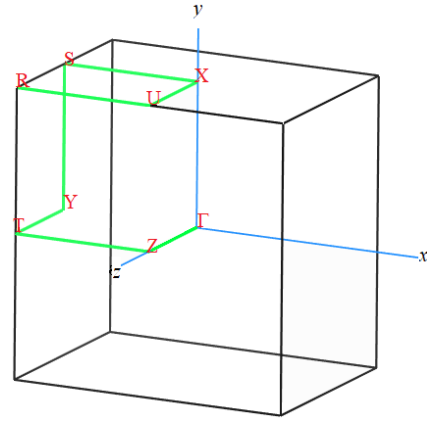
† [m.pawlowski@pw.edu.pl](mailto:m.pawlowski@pw.edu.pl)

‡ [andrii.i.kashuba@lpnu.ua](mailto:andrii.i.kashuba@lpnu.ua)



**Table 1** – Structure parameters of  $\beta$ -Ag<sub>8</sub>GeSe<sub>6</sub> crystal ( $Pma2_1$  – space group)

Methods	$a, \text{\AA}$	$b, \text{\AA}$	$c, \text{\AA}$	$V, \text{\AA}^3$	Ref.
GGA + PBE	7.908322	7.775797	11.005394	676.760	This work
XRD	7.844	7.738	10.92	662.37	[9]
XRD	7.823(1)	7.712(2)	10.885(3)	656.703	[17]
XRD	7.8402	7.7322	10.9118	–	[18, 19]

**Fig. 1** – View of crystal structure of the  $\beta$ -Ag<sub>8</sub>GeSe<sub>6</sub> crystal**Fig. 2** – BZ of the  $\beta$ -Ag<sub>8</sub>GeSe<sub>6</sub> crystal**Table 2** – Atoms position in the  $\beta$ -Ag<sub>8</sub>GeSe<sub>6</sub> crystal

Element	Atom number	$x/a$	$y/b$	$z/c$
Ge	1	0	0.247551	0.518164
Ge	2	0.5	-0.247551	1.018164
Se	1	0.249410	0.750861	0.899941
Se	2	0.250590	-0.750861	1.399941
Se	3	0.749410	-0.750861	1.399941
Se	4	-0.249410	0.750861	0.899941
Se	5	0	0.002139	0.647734
Se	6	0	0.280266	-0.001472
Se	7	0	0.805766	0.248183
Se	8	0	0.486825	0.649148
Se	9	0.5	-0.002139	1.147734
Se	10	0.5	-0.280266	0.498528
Se	11	0.5	-0.805766	0.748183
Se	12	0.5	-0.486825	1.149148
Ag	1	0.205206	0.104198	0.859224
Ag	2	0.197794	0.531362	0.268453
Ag	3	0.198581	0.158629	0.161074
Ag	4	0.294794	-0.104198	1.359224
Ag	5	0.302206	-0.531362	0.768453
Ag	6	0.301419	-0.158629	0.661074
Ag	7	0.705206	-0.104198	1.359224
Ag	8	0.697794	-0.531362	0.768453
Ag	9	0.698581	-0.158629	0.661074
Ag	10	-0.205206	0.104198	0.859224
Ag	11	-0.197794	0.531362	0.268453
Ag	12	-0.198581	0.158629	0.161074
Ag	13	0	0.616266	0.042336
Ag	14	0	0.724870	0.482324
Ag	15	0.5	-0.616266	0.542336
Ag	16	0.5	-0.724870	0.982324

In our calculations, the value  $E_{\text{cut-off}} = 330$  eV was taken for the cutting-off energy of the plane waves (this energy corresponded to minimum value of the total energy). The convergence of the total energy was about  $5 \times 10^{-6}$  eV/atom. Integration over the Brillouin zone (BZ) was performed on a  $2 \times 2 \times 1$  grid of  $\mathbf{k}$  points, using a Monkhorst–Pack scheme [20]. The atomic coordinates and the unit-cell parameters were optimized following a Broyden–Fletcher–Goldfarb–Shanno technique (see information in Table 1 and 2). Optimization was continued until the forces acting on atoms became less than  $0.01$  eV/Å, the maximum displacement less than  $5.0 \times 10^{-4}$  Å, and the mechanical stresses in the cell less than  $0.02$  GPa. Obtained of  $\beta\text{-Ag}_8\text{GeSe}_6$  optimization structure is drawn in Fig. 1 for visualization. Optimization lattice parameters and atom positions are listed in Table 1 and 2. The energy band diagram was constructed using the points  $Z(0, 0, 0.5)$ ,  $T(-0.5, 0, 0.5)$ ,  $Y(-0.5, 0, 0)$ ,  $S(-0.5, 0.5, 0)$ ,  $X(0, 0.5, 0)$ ,  $U(0, 0.5, 0.5)$ ,  $R(-0.5, 0.5, 0.5)$  and  $\Gamma(0, 0, 0)$  of the Brillouin zone in the reciprocal space (see Fig. 2).

### 3. RESULTS AND DISCUSSION

The electron energy band structure building along the highly symmetrical lines of the BZ (see blue lines in Fig. 3) is shown in Fig. 3. On this figure, the red line corresponded to the Fermi level. This means that the energy on the band structure is counted from the Fermi level. As can see in Fig. 3, the higher position of the energy level of the valence band is localized in the  $\Gamma$ -point of BZ. Also, the lower position of the conduction band is localized in the  $\Gamma$ -point of BZ, too. The smallest band gap of  $\beta\text{-Ag}_8\text{GeSe}_6$  crystal corresponds to the difference between these energy positions and was equal to  $0.85$  eV (also see Table 3). As results, the band gap of  $\beta\text{-Ag}_8\text{GeSe}_6$  crystal is found to be of direct type. Comparing the obtained theoretical results with the known other data is listed in Table 3.

In the next step of this studies need to understand the nature of these energy bands. This problem can be resolved by using an analysis of the density of states and their partial contributions (see Fig. 4).

The analysis of the partial contributions of individual levels to the function of the total density of states can be summarized as follows:

1. Energy bands in the ranging from  $-9$  to  $-7$  eV are formed by  $s$ -states of Se.
2. Energy bands in the ranging from  $-15$  to  $-12$  eV are formed by  $s$ -states of Ge.
3. Top of the valence band is composed of the  $d$ -states of Ag, and  $p$ -states of Ag and Se.
4. Bottom of the conduction band is composed of the  $s$ - and  $p$ -states of Ag.

Such contribution is caused by the highest relative content of silver and selenium atoms in  $\beta\text{-Ag}_8\text{GeSe}_6$ . The smaller content explains the smallest partial DOS of germanium in the formula unit  $\beta\text{-Ag}_8\text{GeSe}_6$ .

As result, we assume that the direct band gap transition (see discussed above) in  $\beta\text{-Ag}_8\text{GeSe}_6$  can be formed by the Ag-Se links. Also, the hybridization of electronic states in the energy ranges close to the energy gap  $E_g$  is observed. This manifests itself in similar partial DOS maxims (see energy range of the top valence and bottom conduction bands in Fig. 4). This can affect the electron

conductivity of the  $\beta\text{-Ag}_8\text{GeSe}_6$  crystal because the electrons of the most numerous silver and selenium atoms form mainly the electronic states [11, 21].

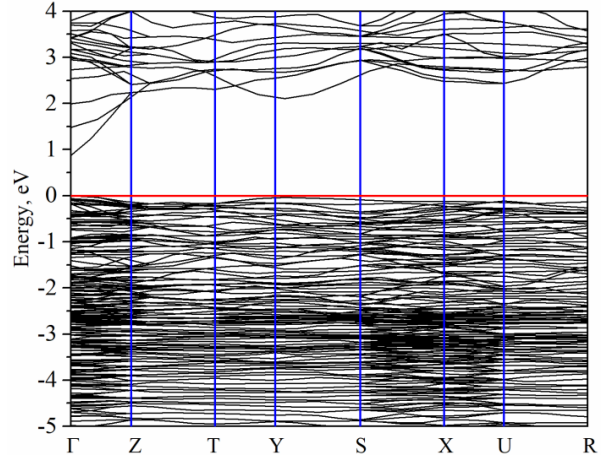


**Fig. 3** – Electron band energy structure of the  $\beta\text{-Ag}_8\text{GeSe}_6$  crystal

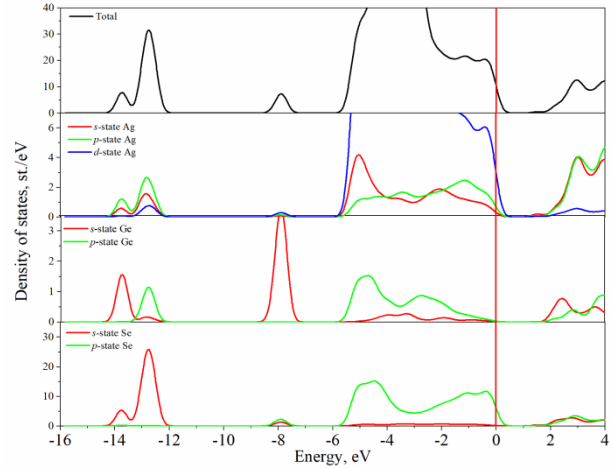


**Fig. 4** – Total and partial densities of states of  $\beta\text{-Ag}_8\text{GeSe}_6$  crystal calculated in the GGA+PBE approximation (vertical red line correspondent to Fermi level)

In addition, the behavior of the energy bands near the band gap shows high anisotropy  $E(\mathbf{k})$  (see Fig. 3). Also, this behavior ( $E(\mathbf{k})$ ) for the valence and conduction bands is different. The valence complex top is flatter than the bottom of conductivity bands. This is explained by the fact that holes can be less mobile than electrons. This behavior is caused by the inverse relationship between the effective mass ( $m$ ) of the electron ( $m_e$ )/hole ( $m_h$ ) and the spread  $E(\mathbf{k})$  of energy levels [22]:

$$\frac{1}{m} = \frac{4\pi^2}{h^2} \frac{d^2 E(k)}{dk^2}, \quad (1)$$

where  $h$  is the Planck constant, and  $E(\mathbf{k})$  is the dependence of the band energy  $E$  on the electron wave vector  $\mathbf{k}$ .

The electron conductivity of materials is one of the important parameters for their practice area application use. According to the semiconductor theory [22] the specific conductivity ( $\sigma$ ) of a material is dependent on the charged particle's mobility ( $\mu$ ),

$$\sigma = nq\mu, \quad (2)$$

where  $q$  is the particle's charge and  $n$  is the charged particle's concentration.

The electron mobility  $\mu$  is can be presented by the following relation [25, 26]:

$$\mu_i = \frac{q\tau_i}{m^*}, \quad (3)$$

where  $\tau_i$  is the relaxation time, which is inversely proportional to the ionized impurity concentration  $n_i$ ,

$$\tau_i \propto n_i^{-1} T^{3/2}, \quad (4)$$

where  $T$  is the thermodynamic temperature. At this time, the electron mobility  $\mu$  satisfies the following relation:

$$\mu \propto \frac{qT^{3/2}}{m^* n_i}, \quad (5)$$

As can see from Eqs. (2) and (5), information about effective masses of electrons and holes need for analysis of the basic thermoelectric properties. The effective masses of electrons and holes in the  $\beta$ -Ag<sub>3</sub>GeSe<sub>6</sub> crystal have been calculated by utilizing the Effective Mass Calculator [23]. The calculated effective masses are presented in Table 3. The obtained absolute value of the  $|m|$  for the conduction band ( $\sim 0.7m_0$ ) is lower than that for the valence band ( $\sim 1.4m_0$ ). The same results were observed for other types of argyrodites in Refs. [10, 21].

**Table 3** – Band gap ( $E_g$ ) and effective mass of the electron ( $m_e$ ) and hole ( $m_h$ ) of the  $\beta$ -Ag<sub>3</sub>GeSe<sub>6</sub> crystal in  $\Gamma$  point of BZ ( $m_0$ - mass of free electron)

$E_g$ , eV	Effective mass		Ref.
	$m_e/m_0$	$m_h/m_0$	
0.85	0.69466	-1.43341	This work
0.85	–	–	[9]
0.87	–	–	[24]

Analysis of Eqs. (2) and (5) show that the electron mobility and conductivity are higher than hole mobility and conductivity ( $|m_h|/|m_e| > 1$ ) for the studied compound, and increase with increasing temperature ( $\mu \sim T^{3/2}$ ) and decrease with increasing carrier concentration ( $\mu \sim n_i^{-1}$ ). Also, in Refs. [10, 27-30] was quoted that the effective mass of the electron is about  $0.16m_0$  and  $2.0m_0$  for  $n$ -type and  $p$ -type conduction's, respectively. Based, on these results we assumed that the  $\beta$ -Ag<sub>3</sub>GeSe<sub>6</sub> is a semiconductor with  $n$ -type conductivity.

One of the main thermoelectric parameters is the Seebeck coefficient [31], which is proportional to the effective mass  $m$ , temperature  $T$ , and the inverse charge carrier density  $n^{-2/3}$ .

$$\alpha = \frac{2k_B^2}{3e\hbar^2} m^* T \left( \frac{\pi}{3n_i} \right)^{2/3}, \quad (6)$$

where,  $k_B$  is Boltzmann constant,  $e$  is the electron charge and  $\hbar$  is Planck constant. The large Seebeck coefficient is expected in material possessing large effective mass and small carrier concentration (see Eq. (6)).

To obtain the Seebeck coefficient ( $\alpha$ ) of  $\beta$ -Ag<sub>3</sub>GeSe<sub>6</sub> crystal need to have a carrier concentration close to its optimum. Using well-known relations (7)-(9) of the semiconductor theory can be calculated carrier concentration of  $\beta$ -Ag<sub>3</sub>GeSe<sub>6</sub> crystal.

$$n_e = 2 \left( \frac{m_e k_B T}{2\pi\hbar^2} \right)^{3/2} \cdot \exp\left( \frac{-(E_c - E_F)}{k_B T} \right), \quad (7)$$

$$n_h = 2 \left( \frac{m_h k_B T}{2\pi\hbar^2} \right)^{3/2} \cdot \exp\left( \frac{-(E_F - E_v)}{k_B T} \right), \quad (8)$$

$$n_i = \sqrt{n_e \cdot n_h}. \quad (9)$$

In Eqs. (7) and (8),  $E_F$  is the position of the Fermi level,  $E_c$  – bottom of the conduction band, and  $E_v$  – top of the valence band.

The temperature behavior of carrier concentration ( $n$ ) calculated by Eq. (9) is shown in Fig. 5. As can see from Fig. 5, the optimal carrier concentration for  $\beta$  modification of the Ag<sub>3</sub>GeSe<sub>6</sub>, which we used for calculations of the Seebeck coefficient, is between  $5 \cdot 10^{14}$ – $5 \cdot 10^{16}$  cm<sup>-3</sup>. In literature was quoted about experimental studies of the Seebeck coefficient ( $\sim 200$   $\mu$ V/K at room temperature) [8, 9]. From the temperature behavior of the Seebeck coefficient with different carrier concentration (see Fig. 6) was established that the optimal carrier concentration is  $1.75 \cdot 10^{16}$  cm<sup>-3</sup> at room temperature. This concentration shows a good correlation with the value obtained from the temperature behavior of carrier concentration (see Fig. 5). The decrease of the Seebeck coefficient  $|\alpha|$  is observed when the carrier concentration increases (see Fig. 6). For every carrier concentration the absolute value of Seebeck coefficient  $|\alpha|$  increases with the increase in temperature (see Fig. 6). These features are in agreement with Eq. (6). Also, Ref. [10] was quoted that the optimum carrier concentration for  $n$ -type argyrodites is less than  $10^{19}$  cm<sup>-3</sup>, while  $p$ -type needs  $10^{20}$  cm<sup>-3</sup> or higher. The obtained value of optimum carrier concentration ( $1.75 \cdot 10^{16}$  cm<sup>-3</sup> at room temperature) confirms that the  $\beta$ -Ag<sub>3</sub>GeSe<sub>6</sub> crystal shows  $n$ -type conductivity.

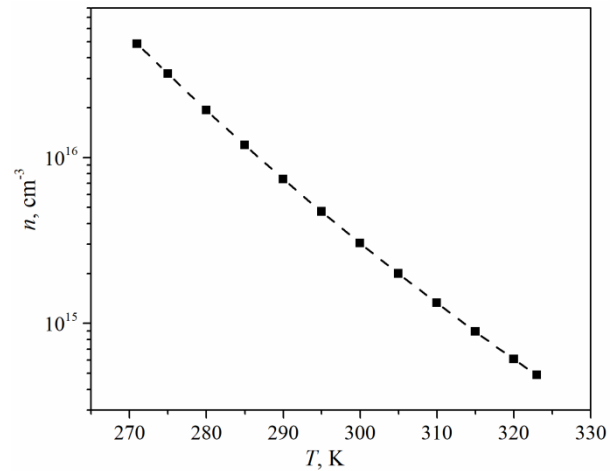


**Fig. 5** – Temperature behavior of carrier concentration of  $\beta$ -Ag<sub>3</sub>GeSe<sub>6</sub> crystal



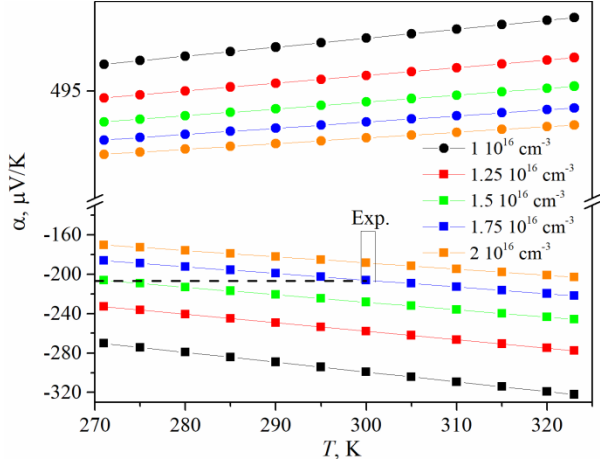


**Fig. 6** – Dependence of Seebeck coefficient  $\alpha$  on temperature for  $\beta$ -Ag<sub>8</sub>GeSe<sub>6</sub> crystal with different carrier concentration (see legend on figure). Circle: for  $p$ -type conductivity, square:  $n$ -type conductivity

Afterward, the power factor  $PF$ , as the main thermoelectric value, may be calculated using the Eq. (10). To obtain the thermoelectric figure of merit  $zT$  (see Eq. (11)) of material has to know the coefficient of thermal conductivity  $\kappa$  ( $\kappa = \kappa_e + \kappa_{ph}$ ). The value of  $\kappa$  is a sum of the corresponding electron and phonon components. The coefficient of electron thermal conductivity  $\kappa_e$  of  $\beta$ -Ag<sub>8</sub>GeSe<sub>6</sub> is determined using the Wiedemann-Franz Law (see Eq. (12)).

$$PF = \alpha^2 \sigma. \quad (10)$$

$$zT = \frac{\alpha^2 \sigma T}{\kappa}. \quad (11)$$

$$\kappa_e = L\sigma T. \quad (12)$$

where,  $L$  is the Lorenz number.

But, for obtaining phonon components of thermal conductivity need information about phonon energy spectra. In this work, we do not study the temperature behavior of the figure of merit and phonon components of thermal conductivity.

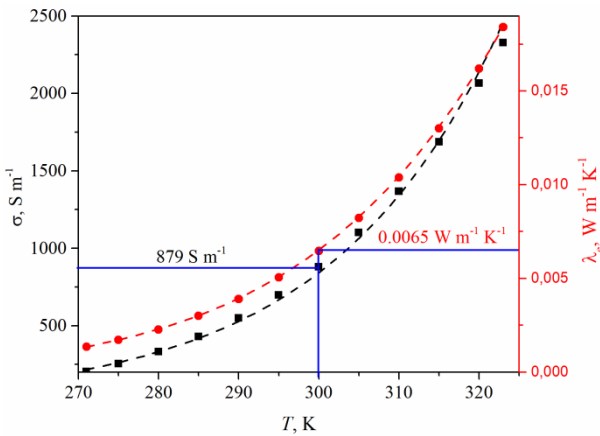


**Fig. 7** – Temperature behavior of electric conductivity (black) and electron components of thermal conductivity (red) for  $\beta$ -Ag<sub>8</sub>GeSe<sub>6</sub> crystal. Blue marks are corresponding to the value at room temperature

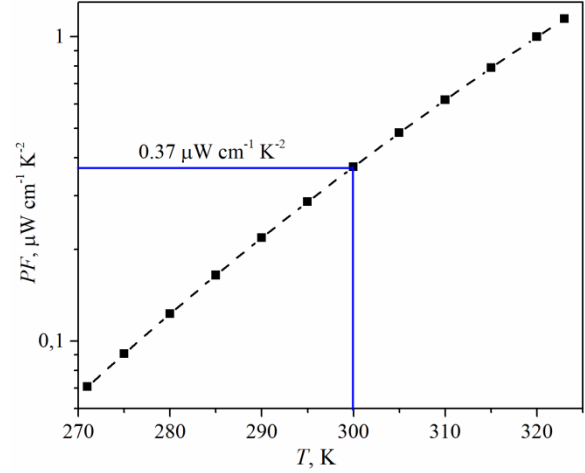


**Fig. 8** – Temperature dependence of power factor for  $\beta$ -Ag<sub>8</sub>GeSe<sub>6</sub> crystal. Blue mark is corresponding to the value at room temperature

Fig. 7 and 8 show the temperature behavior of electric conductivity (calculated using Eq. (2)), electron components of thermal conductivity (Eq. (12)) and power factor (Eq. (10)). For all these parameters show increase behavior with increasing temperature. Comparing the theoretical results of thermoelectric properties with the experimental data is listed in Table 4.

#### 4. CONCLUSION

In this work, theoretical studies of the electron energy spectrum, the density of states, and related with them thermoelectric properties for the  $\beta$ -Ag<sub>8</sub>GeSe<sub>6</sub> crystal have been calculated using the GGA + PBE approximations. Based on the electron energy structure has been established that the smallest optical band gap is localized at the  $\Gamma$ -point of the BZ and corresponds to direct optical transitions. The absolute value of the effective mass of the electron ( $\sim 0.7m_0$ ) and hole ( $\sim 1.4m_0$ ) was calculated based on the results of the electronic structure. The electron mobility and conductivity ( $|m_h|/|m_e| > 1$ ) for the studied compound. Dispersion behaviors of electron energy level are discussed based on results of effective masses study. Based on this calculation, the carrier concentration is calculated as a function of temperature. Also, the Seebeck coefficient is calculated as a function of carrier concentration and temperature for  $n$ - and  $p$ -type conductivity. The decrease of the Seebeck coefficient  $|\alpha|$  is observed when the carrier concentration increases and increases with the temperature increase. Optimal value of the carrier concentration ( $1.75 \cdot 10^{16} \text{ cm}^{-3}$ ) obtained by comparisons of the calculated values with known experimental results. The dependence of the electric conductivity, electron components of thermal conductivity and power factor as a function of temperature are obtained. Correlate analysis of the main thermoelectrically properties shows high coincide. As result, this method of calculation can be used for the ability to determine the electronic and thermoelectric characteristics of materials.

**Table 4** – Thermoelectric properties of the  $\beta$ -Ag<sub>8</sub>GeSe<sub>6</sub> crystal at room temperature (300 K). Italic value was estimated from the figure

$n \cdot 10^{16}, \text{cm}^{-3}$	$\mu, \text{cm}^2 \text{V}^{-1} \text{s}^{-1}$	$\sigma, \text{S m}^{-1}$	$\alpha, \mu\text{V K}^{-1}$	$PF, \mu\text{W cm}^{-1} \text{K}^2$	$\kappa_e, \text{W m}^{-1} \text{K}^{-1}$	Ref.
1.75	3140	879	– 207	0.37	0.0065	This work
1.15	4769	880	– 207	0.38	–	[8]
0.15	663.99	–	– 200	–	–	[9]

**ACKNOWLEDGEMENTS**

This work was supported by the Project of Young

Scientists 0123U100599 of the Ministry of Education and Science of Ukraine.

**REFERENCES**

- M.V. Chekaylo, V.O. Ukrainets, G.A. Il'chuk, Yu.P. Pavlovsky, N.A. Ukrainets, *J. Non-Cryst. Solid.* **358**, 321 (2012).
- A. Kindurys, A. Shileika, *Inst. Phys. Conf. Ser.* **35**, 67 (1977).
- C.W.F.T. Pistorius, O. Gorochoy, *High Temperatures-High Pressures* **2**, 31 (1970).
- O. Gorochoy, *Bull. Soc. Chim. France* **6**, 2263 (1968).
- C. Yang, Y. Xia, L. Xu, Y. Luo, X. Li, Z. Han, J. Cui, *Chem. Eng. J.* **426**, 131752 (2021).
- F.S. Ibrahimova, *Chem. Probl.* **3**, 358 (2019).
- I.D. Alverdiev, S.M. Bagkheri, S.Z. Imamalieva, Yu.A. Yusibov, M.B. Babanly, *Rus. J. Electrochem.* **53**, 551 (2017).
- X. Shen, C.-C. Yang, Y. Liu, G. Wang, H. Tan, Y.-H. Tung, G. Wang, X. Lu, J. He, X. Zhou, *ACS Appl. Mater. Interfaces* **11**, 2168 (2019).
- S. Acharya, J. Pandey, A. Soni, *ACS Appl. Energy Mater* **2**, 654 (2019).
- S. Lin, W. Li, Y. Pei, *Mater. Today* **48**, 198 (2021).
- B. Andriyevsky, I.E. Barchiy, I.P. Studenyak, A.I. Kashuba, M. Piasecki, *Sci. Rep.* **11**, 19065 (2021).
- B. Jiang, P. Qiu, H. Chen, Q. Zhang, K. Zhao, D. Ren, X. Shi, L. Chen, *Chem. Commun.* **53**, 11658 (2017).
- B. Jiang, P. Qiu, E. Eikeland, H. Chen, Q. Song, D. Ren, T. Zhang, J. Yang, B.B. Iversen, X. Shi, L. Chen, *J. Mater. Chem. C* **5**, 943 (2016).
- T.V. Vu, C.V. Nguyen, H.V. Phuc, A.A. Lavrentyev, O.Y. Khyzhun, N.V. Hieu, M.M. Obeid, D.P. Rai, H.D. Tong, N.N. Hieu, *Phys. Rev. B.* **103**, 085422 (2021).
- J.P. Perdew, K. Burke, M. Ernzerhof, *Phys. Rev. Lett.* **78**, 1396 (1997).
- D. Vanderbilt, *Phys. Rev. B.* **41**, 7892(R) (1990).
- D. Carre, R. Ollitrault-Fichet, J. Flahaut, *Acta Cryst.* **B36**, 245 (1980).
- Yu.A. Yusibov, I.D. Alverdiev, F.S. Ibrahimova, A.N. Mamedov, D.B. Tagiev, M.B. Babanly, *Russ. J. Inorg. Chem.* **62**, 1223 (2017).
- Z.M. Alieva, S.M. Bagkheri, I.J. Alverdiev, Yu.A. Yusibov, M.B. Babanly, *Inorg. Mater.* **50**, 981 (2014).
- H.J. Monkhorst, J.D. Pack, *Phys. Rev. B* **13**, 5188 (1976).
- I.V. Semkiv, N.Y. Kashuba, H.A. Ilchuk, A.I. Kashuba, *Low Temp. Phys.* **49**, 1163 (2023).
- A. Kashuba, B. Andriyevskyy, I. Semkiv, L. Andriyevska, R. Petrus, E. Zmiiovska, D. Popovych, *J. Nano-Electron. Phys.* **10** No 6, 06025 (2018).
- A. Fonari, C. Sutton, *Effective Mass Calculator* (2012).
- R. Bendorius, A. Irzikevicius, A. Kindurys, E.V. Tsvetkova, *phys. status solidi (a)* **28**, K125 (1975).
- Z. Yinnu, Y. Jinliang, X. Chengyang, *J. Semicond.* **36**, 012003 (2015).
- J. Liu, Q.-Y. Jiang, S.-D. Zhang, H. Zhang, *Phys. Lett. A* **383**, 125990 (2019).
- B. Jiang, P. Qiu, H. Chen, Q. Zhang, K. Zhao, D. Ren, X. Shi, L. Chen, *Chem. Commun.* **53**, 11658 (2017).
- B.K. Heep, K.S. Weldert, Y. Krysiak, T.W. Day, W.G. Zeier, U. Kolb, G.J. Snyder, W. Tremel, *Chem. Mater.* **29**, 4833 (2017).
- W. Li, S. Lin, B. Ge, J. Yang, W. Zhang, Y. Pei, *Adv. Sci.* **3**, 1600196 (2016).
- S. Schwarzmueller, D. Souchay, D. Guunther, A. Gocke, I. Dovgaliuk, S.A. Miller, G.J. Snyder, O. Oeckler, *Z. Anorg. Allg. Chem.* **644**, 1915 (2018).
- G.J. Snyder, E.S. Toberer, *Nat. Mater.* **7**, 105 (2008).

## Електронна структура та термоелектричні властивості кристала $\beta$ -Ag<sub>8</sub>GeSe<sub>6</sub>, розраховані за методом теорією функціоналу густини

I.V. Семків<sup>1</sup>, Г.А. Ільчук<sup>1</sup>, М. Павловські<sup>2</sup>, Н.Ю. Кашуба<sup>1</sup>, Н.Т. Покладок<sup>1</sup>, А.І. Кашуба<sup>1</sup>

<sup>1</sup> Кафедра загальної фізики, Національний університет «Львівська політехніка», 79013 Львів, Україна

<sup>2</sup> Фізичний факультет, Варшавська політехніка, 00-662 Варшава, Польща

$\beta$ -Ag<sub>8</sub>GeSe<sub>6</sub> кристалізується в ромбічній структурі (просторова група  $Pm\bar{a}21$ ) при кімнатній температурі та досліджується в рамках теорії функціоналу густини. Теоретичні першопринципні розрахунки електронної зонної структури, густини станів, коефіцієнта Зеебека, коефіцієнта потужності, електропровідності та ефективної маси електрона та дірки кристала  $\beta$ -Ag<sub>8</sub>GeSe<sub>6</sub> оцінені за допомогою узагальненого градієнтного наближення (GGA). Було використано функціонал Пердью–Берка–Ернзерхофа (PBE). Ефективна маса електронів і дірок була розрахована на основі електронної зонної структури. Вивчаються та обговорюються коефіцієнт Зеебека, коефіцієнт потужності та електропровідність як функціональна температура. Усі отримані значення при кімнатній температурі порівнюються з відомими експериментальними результатами.

**Ключові слова:** Теорія функціоналу густини, Електронна зона, Ефективна маса, Густина стану, Коефіцієнт Зеебека, Коефіцієнт потужності.